A spectral optical model and updated water clarity reporting tool for Charlotte Harbor seagrasses

L. Kellie Dixon[(1)] and Mike R. Wessel[(2)]

[(1)]Mote Marine Laboratory, 1600 Ken Thompson Pkwy., Sarasota, Florida 34236
[(2)]Janicki Environmental, Inc., 1155 Eden Isle Drive NE, St. Petersburg, Florida 33704

Abstract Seagrass communities are a critical response endpoint used by the Charlotte Harbor National Estuary Program (CHNEP) to manage estuarine water quality in southwest Florida. This paper describes advances made to quantify how primary light attenuation parameters affect the amount and quality of light reaching seagrass target depths through the development of a spectrally explicit optical model, based on partitioned absorption and scattering, and parameterized as a function of color, chlorophyll, and turbidity. The model was developed and validated using empirical data collected throughout CHNEP estuarine management areas from Dona and Roberts Bays to Estero Bay and produces estimates of both attenuation coefficients (K_d) and % Photosynthetically Active Radiation (%PAR) at specified depths. The calibrated model was remarkably well suited to predict water clarity throughout the estuaries and allows for the prediction of K_d without reliance on field light estimates which have been shown to include a great deal of uncertainty in these shallow water estuaries. The model is suitable to replace routine field-based monitoring of light attenuation and model output was easily incorporated into existing statistical tools designed to report on annual water clarity conditions relative to a baseline period (2003-2007) when seagrasses were stable in this estuary.

Keywords Charlotte Harbor, light requirements, optical model, PAR, seagrass, water clarity

Introduction and Background

The Charlotte Harbor estuary, located in southwest Florida, is shallow, subtropical, and connects to the Gulf of Mexico through several passes between barrier islands (McPherson et al. 1996). The 90,650 ha estuary has been divided into 14 segments (Figure 1) of relatively homogeneous seagrass and water quality conditions (JEI 2009); Dona and Roberts Bays (DRB), Upper Lemon Bay (ULB), Lower Lemon Bay (LLB), Tidal Myakka River (TMR), Tidal Peace River (TPR), East Wall (EW), West Wall (WW), Bokeelia (BOK), Cape Haze (CHZ), Pine Island Sound (PIS), Matlacha Pass (MP), Tidal Caloosahatchee River (TCR), San Carlos Bay (SCB) and Estero Bay (EB). Compared to others in SW Florida, the estuary has high levels of colored dissolved organic matter (CDOM) in the upper reaches due to freshwater inflows from the Myakka, Peace and Caloosahatchee Rivers. The lower portions, generally experience higher salinity and higher clarity waters resulting from more direct exchange with the Gulf of Mexico, though some segments (e.g. Lemon Bay and Estero Bay) are more lagoonal.

Corresponding author: L. K. Dixon, lkdixon@mote.org

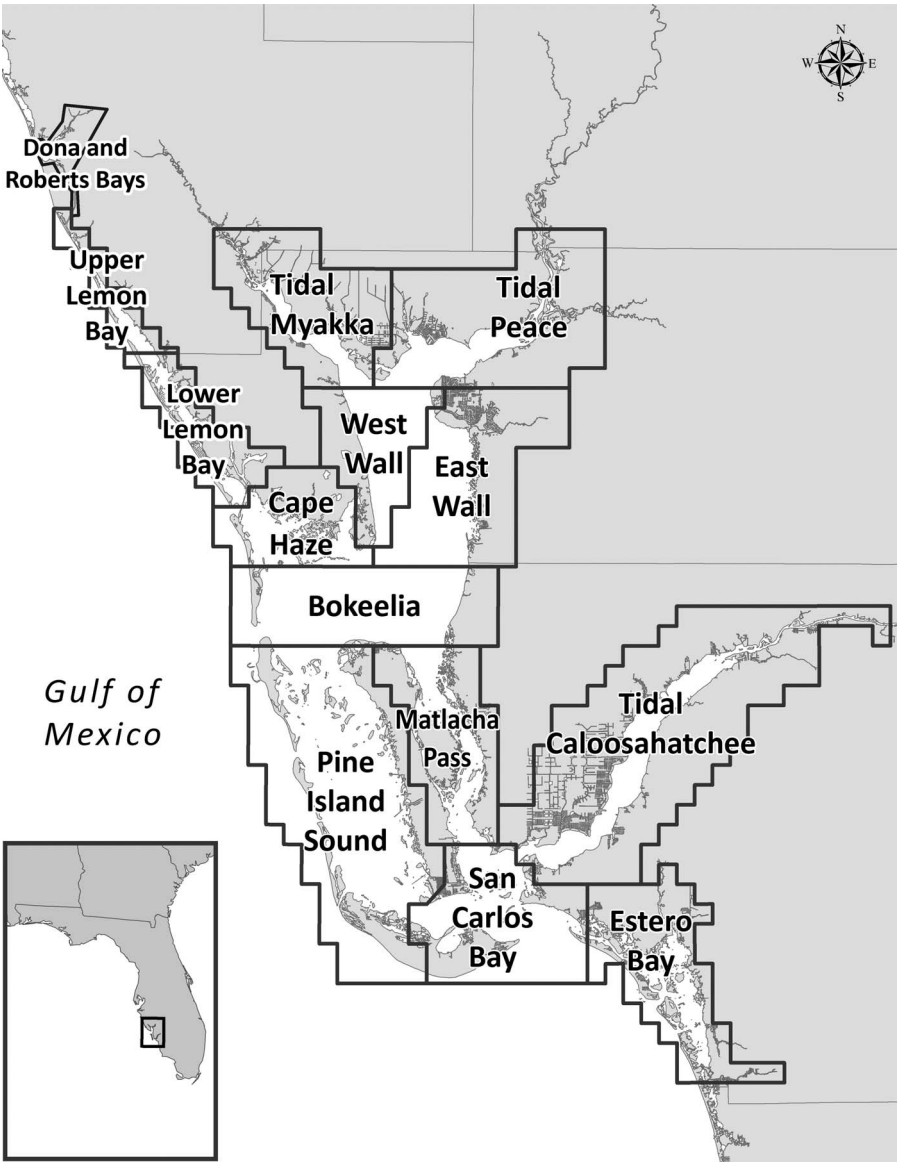

Figure 1. Charlotte Harbor study area and seagrass segments.

The Charlotte Harbor National Estuary Program (CHNEP) manages this region through the implementation of the Comprehensive Conservation and Management Plan (CHNEP 2008) using science-based decision making and management tools. Protection and restoration of seagrass acreage in this productive ecosystem represents a cornerstone of much of the management effort. While mechanistic relationships between water quality, other conditions,

and the living resource requirements of seagrass are not fully understood, the preponderance of evidence suggests that water clarity is a limiting factor in determining the depth distribution, and therefore areal extent, of seagrass.

Management efforts for seagrasses established target seagrass acreages by segment (Janicki et al. 2009) as the greater of either the 1950's baseline acreage (adjusted for non-restorable areas) or the mean of all recent seagrass surveys from 1988, 1994, 1999, 2001, 2004, and 2006. Segments were designated for "Restoration" when recent acreages were less than adjusted baseline and for "Protection" when recent acreages were greater. Seagrass management targets for the highly colored tidal river segments where interpreting aerial photography is difficult (DRB, TMR, TPR, and TCR) were assigned a "Protection" or "Restoration" designation based on regulatory status and local expertise (JEI 2011).

Target depths to achieve desired seagrass cover had been previously established from observed depth distributions in either 1995-2005 or in 2003 (Corbett 2006, Corbett and Hale 2006) and ranged from 0.9-2.4 m. Photosynthetically active radiation (PAR) needed to maintain seagrasses was initially estimated at 25% of immediately subsurface values based on regional literature (Tomasko and Hall 1999, Dixon 2000, Greening and Janicki 2006). Combining target depths and 25% PAR resulted in estimated water clarity targets, measured as vertical diffuse attenuation coefficients of PAR (K_{dPAR}), of 0.6-1.4 m^{-1}. Comparing field measured K_{dPAR} with K_{dPAR} modeled from linear combinations of regression-derived partial attenuation coefficients (McPherson and Miller 1994, Corbett 2006), however, indicated a lack of predictive capacity in the regression relationship (Wessel and Corbett 2009). There were also notable artifacts in observed K_{dPAR} time series attributed to field technique changes.

The most recent seagrass management efforts (JEI 2010, 2011) proposed water clarity targets for light-limited seagrass, on the premise that improving water clarity would result in an increase in the areal extent of seagrasses. By identifying water clarity during a reference period as a target, it was not necessary to explicitly quantify the light requirements of seagrass or the impacts of other potentially limiting factors such as salinity. Segment-specific water clarity targets were ultimately established using selected percentiles of cumulative frequency distribution curves of measured K_{dPAR} during the reference period (2003 – 2007) when seagrass cover was generally acceptable and water clarity data were available. The recently established CHNEP Water Clarity Reporting Tool (JEI 2010, 2011, Wessel et al. 2013) employed a binomial test to evaluate annual distributions of measured K_{dPAR} with respect to that of the reference period for progress towards clarity goals within individual segments.

An apparent optical property, K_{dPAR} is a function not only of the inherent optical properties of absorption and scattering, but is also affected (both positively and negatively) by the angular distribution of light (sky and cloud conditions; sun angle). In addition, field measurements of KdPAR in shallow systems can be "contaminated" by wave climate, bottom reflectance, and other issues beyond the samplers' control.

Comparison of field K_{dPAR} with modeled K_{dPAR} (Dixon et al. 2010) indicated that an existing, spectrally explicit optical model had substantially improved coefficients of determination relative to field observations than did the partial attenuation coefficient approach. In addition, the spectral model approach was spatially consistent over multiple estuarine segments. Given the shallow depths, "bright" sand bottoms in much of the estuary, and difficulties in the field measurement of attenuation coefficients, Dixon suggested that spectrally explicit model estimates may more consistently represent water column attenuators of light compared to actual field measurements of light attenuation. Based on this information, the CHNEP funded the creation of an optical model in which K_{dPAR} could be reproducibly computed from the monitoring parameters of color, chlorophyll *a,* and turbidity. The model was to be calibrated against only the highest quality field measurements of K_{dPAR} made in multiple segments of the CHNEP study area. The calibrated model was then to be applied to the entire body of water quality monitoring data in order to 1) estimate water clarity conditions for each of the estuary segments, 2) evaluate water clarity with respect to a designated reference period judged optimal for seagrasses, and 3) assess changes in water clarity over time.

Materials and Methods

Field and water quality data. Water quality data were available from 1998 through December 2011 for stratified random and fixed stations sampled by the Coastal Charlotte Harbor Monitoring Network and for DRB and ULB sampled by Sarasota County. There were 13,232 samples with complete parametric coverage of color, chlorophyll, and turbidity data. Chlorophyll data were predominantly available as chlorophyll *a*, corrected or adjusted for pheophytin. Turbidity was determined by nephelometry and methodologies were uniform across all data providers. Color values were determined either through visual determination of unfiltered samples as apparent color, or by spectrophotometric determination of absorption on filtered samples (0.45 μm) at 465 nm and reported in platinum cobalt units (PCU). Maximum water quality values recorded were 420 μg L^{-1} Chlorophyll *a*, corrected for pheophytin, 68 NTU of turbidity, 375 PCU of spectrophotometric true color ($Color_{PCU\text{-}465}$), and 507 PCU of visually determined apparent color ($Color_{PCU\text{-}Vis}$).

In association with the water quality monitoring, measurements of PAR irradiance at two or more depths per station were made with quantum sensors exhibiting a spectrally flat response to photons between 400-700 nm. Techniques to collect PAR data have varied over the years. In addition to both single and paired sensors, both flat sensors (2π) measuring irradiance and spherical (4π) sensors measuring scalar irradiance have been used. Experience in SW Florida estuaries (Dixon and Kirkpatrick 1995, Dixon et al. 2010), and literature (Kirk 1994a) indicate that K_{dPAR} determined with 2π sensors is approximately equal to attenuation of scalar irradiance and so no distinction between sensor type was made. When in-air readings were available, multiple readings made with a single sensor were ratio corrected for varying incident irradiance ("air correction"). Values of K_{dPAR} were computed as the negative slope of *ln* (irradiance) as a function of depth.

Model calibration data. Field data for optical model calibration were limited to K_{dPAR} with coefficients of determination (r^2) greater than 0.95 and less than 1.0 (i.e. more than 2 data points), for the r^2 associated with air-corrected K_{dPAR} to be greater than or equal to the r^2 of uncorrected K_{dPAR}, and for the K_{dPAR} of an ambient station to be greater than or equal to 0.20 m^{-1}, the approximate K_{dPAR} of pure water alone. Restricting calibration data to stations with an overall measurement depth greater than 1.5 m improved agreement between modeled and observed K_{dPAR}

by identifying data more likely to have been collected under optically deep conditions (consistent with model assumptions). Calibration data were available in all but two segments and emphasized the estimated K_{dPAR} range of less than 1.6 m^{-1} needed for support of seagrasses. The two segments without data in the calibration were DRB and ULB, where measurement techniques only employed two depths and all r^2 were 1.0. Maximum water quality data associated with the selected field observations (n=445) were absorption coefficient at 440 nm (a_{g440}) of 11.8 m^{-1}, $Color_{PCU\text{-}Vis}$ of 150 PCU, $Color_{PCU\text{-}465}$ of 130 PCU, Chlorophyll *a* of 88.0 µg L^{-1}, and turbidity of 11.1 NTU and a field K_{dPAR} of 2.7 m^{-1}.

Optical model. The empirical optical model to be used originated with equations presented in Kirk (1981, 1984, 1991, 1994b) in which the vertical diffuse attenuation coefficient for a given wavelength ($K_{d\lambda}$) is a function of the cosine (μ_0) of the solar zenith angle, and wavelength-specific total absorption ($a_{t\lambda}$) and scattering (b_λ) coefficients.

$$K_{d\lambda} = (1/\mu_0) * [a_{t\lambda}^2 + (g_1 * \mu_0 - g_2) * a_{t\lambda} * b_\lambda]$$

The empirical model approach has been repeatedly validated and used under a wide range of water quality conditions (Kirk 1981, Kirk 1984, Gallegos et al. 1990, Kirk 1991, Gallegos 1994, Kirk 1994b, Dixon and Kirkpatrick 1999, Gallegos 2001, Gallegos 2005, Gallegos et al. 2006, Johansson 2007, Biber et al. 2008, Johansson et al. 2009, Dixon et al. 2010, Johansson 2012, Dixon 2014). Models based on the solution of radiative transfer equations (Mobley 1994) have also been used to validate the spectral empirical models (Gallegos 2001), resulting in very high and unbiased correlations between the two approaches in optically deep areas. The agreement between empirical and radiative transfer models results further implies that much of the source of scatter between observed and empirically model K_{dPAR} values should be attributed to making observations under conditions not modeled (optically shallow systems, significant amounts of skylight) or to the difficulty of making K_{dPAR} measurements, rather than to bias in the modeling approach. Model outputs retain the assumptions under which they were formulated, simulating $K_{d\lambda}$ under optically deep conditions (i.e. no measurable bottom reflectance) and under direct sunlight only (i.e. direct radiance from the solar disk in the "black" sky, and not including irradiance due to scattered light or skylight from the remaining portion of the hemisphere) (Kirk 1984, Gallegos 1994).

For individual water quality and K_{dPAR} observations, the solar zenith angle was derived from the day of the year, solar declination, station latitude, and recorded time, and was adjusted for the time constant, the offset in minutes between the longitude of the station and the longitude of the eastern boundary of the start of the local time zone (Kirk 1994a). Air mass, the path through the atmosphere that sunlight travels for a given solar elevation relative to when the sun is directly overhead was computed from solar elevation, using an empirical adjustment for a curved rather than a plane-parallel atmosphere (Kasten and Young 1989). Similar computations were used to calculate the zenith angles for maximum solar elevation (solar noon) on individual sampling days. From the solar zenith angle in air, the in-water zenith angle and cosine (μ_0) were computed with Snell's Law and the relative index of refraction between air and water.

To obtain representative spectra of sunlight incident on the water column, the spectral distribution of extraterrestrial radiation (ASTM 2003) was adjusted for the Earth-Sun distance for the day of the year (Kirk 1994a). "Global Tilt" values (spectral radiation from solar disk plus sky diffuse and diffuse reflected from ground on south facing surface tilted 37° from horizontal, under 1.5 SA) (ASTM 2003) were geometrically adjusted to normal values, and using Beer's Law, approximate atmospheric extinction coefficients were computed between adjusted global tilt and solar spectrum at top of atmosphere at the mean Earth-Sun distance (ASTM 2003).

Individual solar elevations, resulting air mass, and derived atmospheric extinction coefficients were used to compute the approximate spectral incident irradiance just below the water surface ($I_{0\lambda}$) for each observation. Resulting PAR (integration of $I_{0\lambda}$ between 400 and 700 nm) resulted in a seasonal range of I_{0PAR} of 1800-2000 µmol m^{-2} s^{-1}, consistent with field observations of in-air

irradiance. Reductions in irradiance due to reflectance at the air-water surface, although a function of solar elevation (Austin 1974, as shown in Kirk 1994b) was considered spectrally flat and neglected.

The optical model was formulated to obtain $a_{t\lambda}$ and b_{λ} as empirical spectral functions of the water quality monitoring parameters that represent the characteristic particulate and dissolved attenuating substances (color, chlorophyll, and turbidity). Total absorption ($a_{t\lambda}$) was partitioned into that attributable to water ($a_{w\lambda}$), chlorophyll or phytoplankton pigments ($a_{ph\lambda}$), non-chlorophyllous particulates or detritus ($a_{d\lambda}$), and dissolved color or *gelbstoff* ($a_{g\lambda}$) with a non-linear wavelength dependence of each term.

$$a_{t\lambda} = a_{w\lambda} + a_{g\lambda} + a_{ph\lambda} + a_{d\lambda}$$

Water absorption spectra were drawn from literature values (Pope and Fry 1997). Values, supplied every 2.5 nm, were splined (Matlab 6.R12) to 2 nm increments. Remaining partitioned absorption coefficients were measured on specialized samples and then quantified as a function of associated water quality values to permit the application of the optical model to existing water quality data. The model is therefore regionally specific, representing the typical CDOM, phytoplankton, and particulates present.

Model formulations. Spectral scans of a_g were performed on samples collected from stations in TMR, TPR, EW, WW, CHZ, and BOK between April 1997 and March 1998 and from additional stations in MP, PIS, and SCB between June and November 1997 (n=137) (Dixon and Kirkpatrick 1999). Samples were filtered through 0.2 micron filters (Sterivex^{TM}). Absorption scans were zeroed at 700 nm where thermal artifacts are minimal and CDOM absorption expected to be absent. A negative exponential function of wavelength (Bricaud et al. 1981), a_g is generally computed using both a reference value and a spectral slope determined at low wavelengths where absorption is maximized. The exponential fit to spectral a_g determined in one wavelength region, however, is imperfect in other spectral regions. As a result of the typically high concentrations of CDOM in Charlotte Harbor waters, little light penetrates the water column at low wavelengths and absorption due to water alone limits penetration for longer wavelengths. Minimum $K_{d\lambda}$ values and maximum resulting %PAR penetrating the water column occurs near mid spectra. Accordingly, the wavelength of the reference a_g (550 nm) and the spectral range used to derive spectral slopes (S_g, 500-600 nm) was selected to optimize model agreement in the region of minimum K_{dPAR} and maximum PAR. Information on a_{g440} was retained for comparison with other literature.

Monitoring programs differed in the technique of color analysis, resulting in two methods of computing reference a_{g440} and a_{g550} from reported color values. Spectrophotometric color (based on absorption at 465 nm) was back transformed from PCU to the a_{g465} of platinum cobalt standards (Mote Marine Laboratory unpublished data) as:

$$a_{g465} = \text{Color}_{\text{PCU-465}} / 16.02895$$

The resulting a_{g465} of samples was converted to a_{g440} based on the nearly linear relationship of a_{g465} and a_{g440} in the 1997-1998 ambient samples of:

$$a_{g440} = 1.58595463 * a_{g465}{}^{0.95895333}$$

Apparent color determined visually was converted to a_{g440} based on concurrent scans with measured a_{g440} and visual color determinations of the 1997-1998 samples.

$$a_{g440} = 0.02842795 * \text{Color}_{\text{PCU-Vis}}{}^{1.18483956}$$

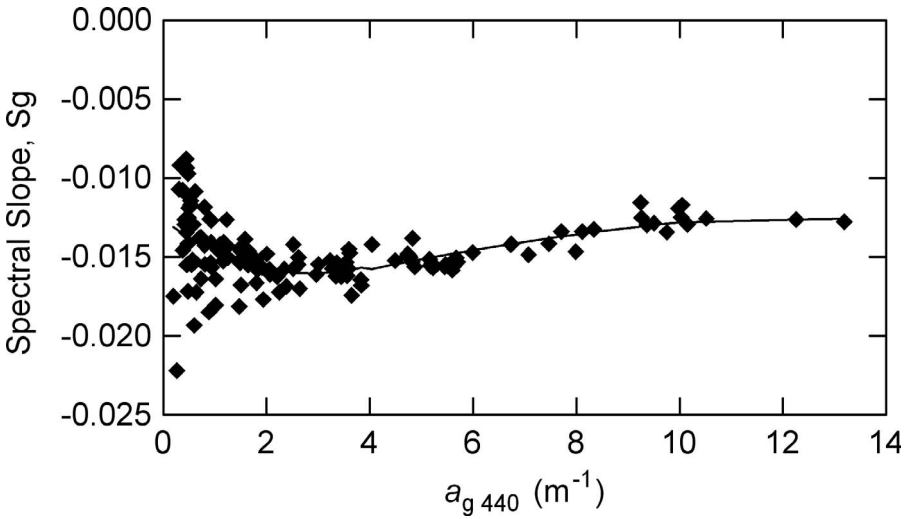

Figure 2. Spectral slope, S_g, 500-600 nm, as a function of observed a_{g440} for 1997-1998 data at selected stations.

Subsequently, a_{g550} was computed from either type of derived a_{g440} using a_{g440} and a_{g550} relationships of the 1997-1998 samples and limiting results to 0.00 m^{-1} and greater:

$$a_{g550} = \mathrm{MAX}(0, 0.00771348 * (a_{g440})^2 + 0.16458477 * a_{g440} - 0.01053129)$$

Spectral slopes, S_g, of dissolved color were determined on *ln*-transformed a_g data between 500-600 nm from the 1997-1998 samples and also modeled as a function of a_{g440}. The function was complex (Figure 2) and was fit as a three part equation to mimic observed slopes and to reasonably account for slopes at color values higher than observed in the calibration data.

$$\begin{aligned} S_g = {} & \text{If } a_{g440} <= 4.0, \\ & \quad 0.00040224 * {a_{g440}}^2 - 0.00232357 * a_{g440} - 0.01267477 \\ & \text{If } a_{g440} > 4.0 \text{ and } a_{g500} <= 13.5, \\ & \quad -0.00002682 * {a_{g440}}^2 + 0.00087068 * a_{g440} - 0.01882298 \\ & \text{If } a_{g440} > 13.5 \\ & \quad -0.01177 \end{aligned}$$

Relationships between a_{g440} and S_g were determined from samples with a maximum a_{g440} of 13.1 m^{-1} (400 PCU for $Color_{PCU\text{-}Vis}$, and 260 PCU for $Color_{PCU\text{-}465}$), while samples to be modeled for status evaluations were as high as 33.7 m^{-1} (507 PCU for $Color_{PCU\text{-}Vis}$, and 375 PCU for $Color_{PCU\text{-}465}$). Slopes for samples with color values outside the available calibration range were limited to that observed for the highest calibration samples. Slopes were somewhat smaller than other literature references due to the longer wavelengths used for slope determination but comparable to those noted for similar highly colored waters (Gallegos 2005). The range in slopes at low a_{g440} values was likely indicative of CDOM from multiple sources. Other numeric models of a_g were also explored (Twardowski et al. 2004) but offered no improvements in fit across larger wavelength ranges. Absorption due to color, a_g, was then computed as:

$$a_{g\lambda} = a_{g550} * e^{[Sg * (\lambda - 550)]}$$

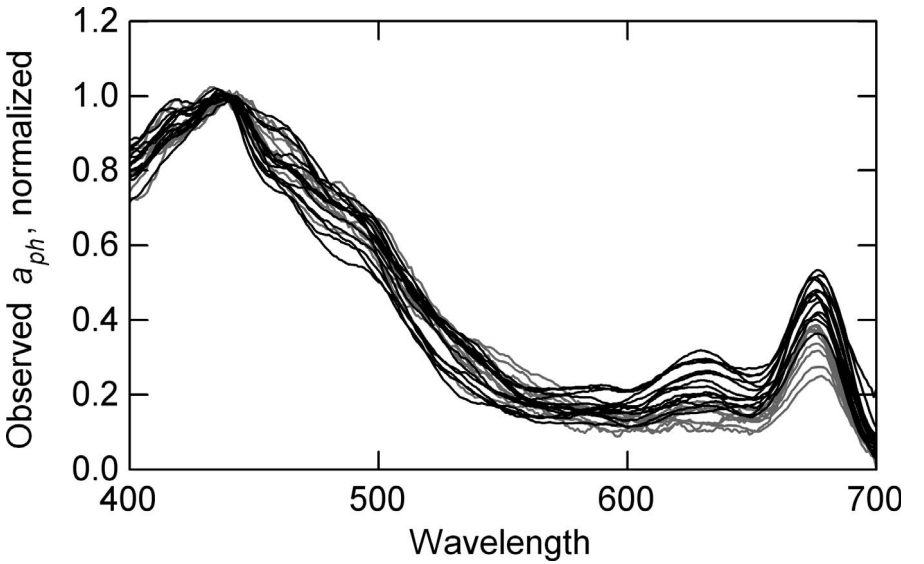

Figure 3. Chlorophyll absorption spectra, a_{ph}, normalized to a_{ph440} indicating remaining seasonal variation; May-grey, August-black.

Absorption coefficients due to chlorophyll pigments and detritus were determined on the 1997-1998 samples by the method of Kishino (1985), Butler (1962), and Cleveland and Weidemann (1993). Samples (n=129) were filtered through glass fiber filters (GF/F, 0.7 μm), scanned for absorbance relative to a clean filter, extracted with methanol to remove pigments, and rescanned. Absorption coefficients were computed from optical density by multiplying by 2.303 and dividing by path length (based on filter clearance area and volume filtered). Path amplification (*Beta* factors; representing the additional absorption that occurs due to the increased path length of light and opportunities for absorption as light transits the filter) were set at 1.0 until model calibration. Chlorophyll absorption was computed as the difference between the pre- and post-solvent extraction scans, while detrital absorption was that of the depigmented scan.

Typically, available spectral absorption profiles of chlorophyll are normalized to absorption at a given wavelength (such as 440 nm), and a single normalized absorption spectra computed. The mean spectra is then scaled by the chlorophyll-specific absorption at 440 nm (a^*_{ph440}), itself computed via regression of a_{ph440} as a function of chlorophyll content determined either spectrophotometrically or fluorometrically (Arar and Collins 1997, APHA 2005). Collectively, however, normalized spectra displayed considerable seasonal variation (Figure 3) related to chlorophyll concentration, likely attributable to varying phytoplankton species. Accordingly, chlorophyll absorption for each wavelength was individually modeled as a series of power relationships of chlorophyll (Figure 4). Coefficients of determination, r^2, were generally 0.9 or above, with the form as:

$$a_{ph} = \mathrm{C} * \mathrm{Chl}^{\mathrm{B}}$$

The modeled chlorophyll absorption, although less variable than that of the original data (Figure 5), did maintain some portion of the seasonal variation in normalized absorption profiles with fits substantially improved in the low absorption region of >500 nm. The formulae for a_{ph} were developed with chlorophyll values as high as 143 μg L^{-1}, relative to a maximum of 420 μg L^{-1} in the data to be modeled. Power relationships prevented sample chlorophyll values greater than calibration data from resulting in lower computed absorption. Similar to a_w values, C and B coefficients were held as tabular data within the model.

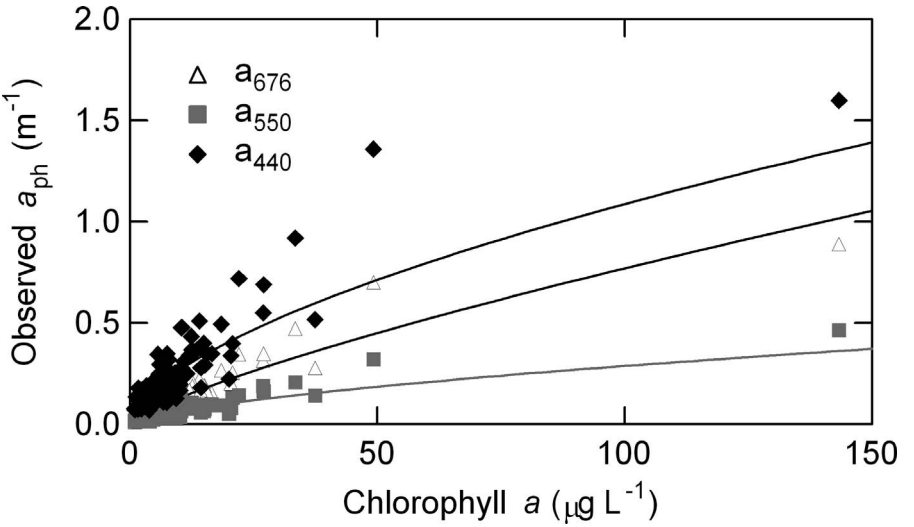

Figure 4. Selected wavelengths of the direct model of chlorophyll absorption, a_{ph}; 440, 550, and 676 nm.

Spectral absorption coefficients due to detritus (a_d) were obtained from the post-solvent extraction scans of particulates described above. Detrital absorption includes not only that due to suspended mineral and organic detrital particles, but also that due to the remaining structural components of de-pigmented phytoplankton. Detrital absorption is well represented by a negative exponential similar to that of dissolved color (Bricaud et al. 1981). Continuing to maximize model

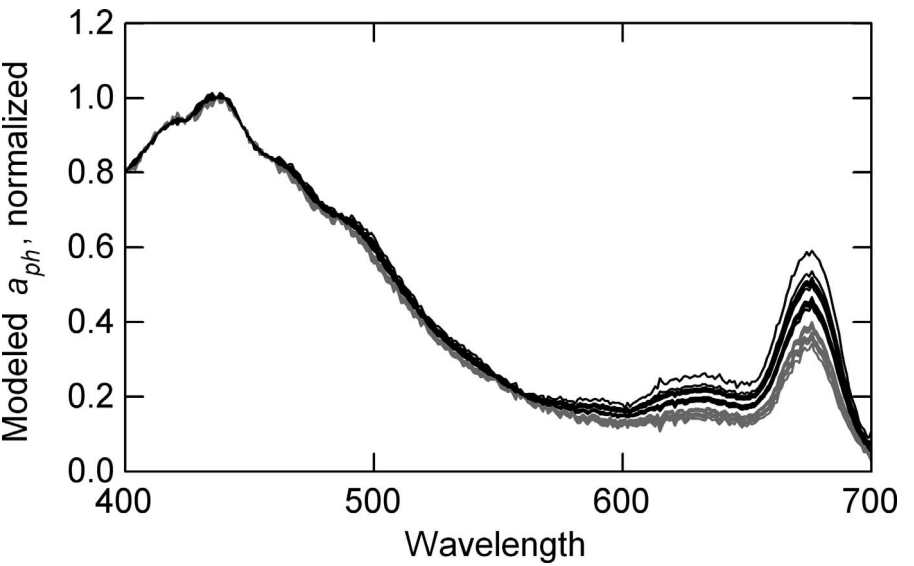

Figure 5. Modeled chlorophyll absorption, a_{ph}, normalized to a_{ph440}; May-grey, August-black.

accuracy in the region of low overall attenuation, spectral slopes were determined from 500-600 nm, using a reference wavelength of 550 nm:

$$a_d = a_{d550} * e^{[Sd*(\lambda - 550)]}$$

Reference a_{d550} and spectral slopes were computed as the optimal function of available water quality parameters and were significant functions of both turbidity and dissolved color, a_{g440}, again limiting a_{d550} to 0.0 m^{-1} or greater.

$$a_{d550} = \text{MAX}(0,-0.037345 + 0.026239 * \text{Turbidity} + 0.012644 * a_{g440})$$
$$S_d = -0.00000419 * (a_{g440})^2 + 0.00024174 * a_{g440} - 0.01120509$$

Spectral slopes, S_d, exhibited a shallow slope with a_{g440} but were not a significant function of turbidity. Maximum turbidity data and a_{g440} data used to develop the empirical formula of a_d were 16.9 NTU and 10.5 m^{-1}, respectively, relative to 68 NTU and 33.7 m^{-1} in the data set to be modeled. The color dependence of both a_{d550} and detrital spectral slope, S_d, indicated that precipitated humic and fulvic acids (components of dissolved color) likely form the basis of much of the turbidity and particulates in the Charlotte Harbor system.

Particulate scattering is reported to be best described as a direct function of turbidity (Morel and Gentili 1991, Gallegos et al. 2008) with an inverse wavelength dependent term and scattering at a reference wavelength approximately equal to 0.92 to 1.1 times turbidity (Kirk 1994a). Exponents to the normalized wavelength term (Morel 1973, DiToro 1978, Gallegos et al. 2009) range between 0.8 and 1.1, with an occasional dependence on color. Scattering due to water alone (Buiteveld et al. 1994) was 300-7000 times smaller than that estimated from particulates and was subsequently ignored. Results from the Charlotte Harbor model were not strongly dependent on the precise scattering formula, but gave marginally better agreements using values of:

$$b_\lambda = 1.1 * \text{Turbidity} * (555/\lambda)^{0.8}$$

For model calibration, a_t and b were computed from the water quality data as described above, μ_0 was computed for the time of sampling, and wavelength-specific $K_{d\lambda}$ computed using the optical model formulation. Spectral incident irradiance ($I_{0\lambda}$) at the time of collection was then attenuated at each wavelength, using the appropriate $K_{d\lambda}$, to compute $I_{z\lambda}$, at both the minimum (z_1) and the maximum (z_2) depths at which PAR measurements were made.

$$I_{z\lambda} = I_{0\lambda} * e^{(-K_{d\lambda} * z)}$$

The resulting modeled irradiance at z_1 and z_2 was then integrated from 400-700 nm to simulate the PAR readings obtained by field instrumentation. With strong spectral structure in $K_{d\lambda}$, declines of 10-20% in K_{dPAR} can be expected with increasing depth due to the progressive removal of the more strongly attenuated wavelengths. Modeling K_{dPAR} between the depths actually used for field observations was expected to provide a more appropriate comparison and also emphasizes that modeled K_{dPAR} is strictly applicable only to the depths between which it was derived. Modeled K_{dPAR} was computed as

$$\text{Modeled } K_{dPAR} = -ln(\Sigma[I_{z2\lambda}] / \Sigma[I_{z1\lambda}]) / (z_2 - z_1)$$

Optical model calibration consisted of iteratively varying model parameters and maximizing the agreement between modeled and field-observed K_{dPAR}. Comparisons were conducted using a Line of Organic Correlation (LOC) (Helsel and Hirsch 2002) in which potential errors are assumed in both the *x*- and *y*-dimensions. A desired slope for the relationship would be between 0.8-1.2, with an intercept within ± 0.20 m^{-1}, the approximate theoretical K_{dPAR} of pure water alone

between 0.0 and 0.5 m. In addition, residuals were examined to minimize distribution with respect to water quality variables.

Modeled results proved relatively insensitive to the range of literature values for coefficients g_1 and g_2 and so values of 0.473 and 0.218, empirically determined for the midpoint of the euphotic zone (Kirk 1994a), were used. Other model parameters to be adjusted during calibration were path amplification factors applied to the absorption due to chlorophyll and detritus. The a_d and a_{ph} quantities measured by the filter pad method are considered to be biased high relative to the same materials in suspension as result of increased scatter and additional opportunities for absorption as light transits the filter pad (Bricaud and Stramski 1990, Nelson and Robertson 1993). Factors can be either a fixed or absorption-dependent quantity, can vary by particle size or phytoplankton species, and can range by a factor of 6 or more (Mueller et al. 2003), but are generally used to reduce computed partial absorptions for materials in suspension.

As no direct measurements of suspensions or path amplification were available for Charlotte Harbor particulates, factors were adjusted to optimize modeled K_{dPAR} results with respect to field observations and to remove parameter-dependent distributions in residuals. Initial residuals displayed strong positive correlations (model underestimation) with both turbidity and chlorophyll concentrations. Rather than reducing computed a_d and a_{ph} by a *Beta* factor, enhancement factors of 1.6 and 1.8 for a_d and a_{ph}, respectively, were required to minimize residuals across the range of available water quality data. Absorption dependent factors (Mueller et al. 2003) did not substantively improve model fit relative to fixed factors. Absorption due to dissolved color is not typically accorded a *Beta* adjustment or enhancement as a_g is measured directly on filtered samples. Model residuals with respect to a_{g440} computed from color analyses, however, were similarly distributed until an enhancement factor of 1.5 was applied to a_{g440}.

Although the actual times of field measurements and resulting sun angles were used for calibration, model application for clarity trend assessment was conducted at local noon on the date of sample collection and K_{dPAR} was modeled between the surface and the segment-specific seagrass target depths. The use of the standardized conditions and local noon produced attenuation coefficients that were independent of station order, could be considered a daily maxima for the given water quality parameters and direct sunlight assumptions, and were unaffected by time of day, cloud cover, segment or measurement depth, or bottom type, responding only to water column attenuators.

Model application. Following optical model calibration, modeled K_{dPAR} was computed from all available water quality data, using segment-specific seagrass target depths as z_2, and with z_1 set to 0.0 m. The solar elevation at local noon was used for each date, minimizing K_{dPAR} for the given date and water quality, and removing time biases in sampling. Model results provided K_{dPAR} values independent of weather (wind, clouds), overall water depth, and bottom type.

Water Clarity Reporting Tool. The application of the Water Clarity Reporting Tool (Wessel et al. 2013) was identical in approach to that earlier applied to *field* measurements of K_{dPAR}, but in this updated instance was applied to *modeled* K_{dPAR} values. Data were limited to K_{dPAR} computed from randomized stations, sampled as part of the Coastal Charlotte Harbor Monitoring Network, and the randomized stations of DRB and ULB. The density of data was reviewed to avoid bias from a changing number of stations or missing sampling periods. The TCR segment changed from five monthly stations to three during 2006, but the three samples continued to extend over the entire segment. There were very few data from MP in 2003 and so the reference period for this segment was 2004-2007. Appropriate application of the Reporting Tool in the future depends on maintaining a similar density, frequency, and seasonal timing of sampling efforts.

The distribution of K_{dPAR} during the reference period was considered to be most representative of the target light requirements of seagrasses in each segment. Selected percentiles (30^{th}, 70^{th}) from the reference distribution were chosen as benchmark points. As described in Wessel et al. (2013), the

Table 1. Water clarity scores, categories, and colors: Declining (D), Caution (C), Stable (S) and Improving (I) categories with color codes of dark grey (red), light grey (yellow), and white (green).

Score	Protection	Restoration
-2	C, D*	D
-1	C	C
0	S	C
1	S	C
2	S	I

binomial test (Wackerly et al. 1996) was used to establish a scoring method to evaluate each year's water clarity data relative to the benchmark points. If more than 30% of the K_{dPAR} measurements were significantly below the 30% benchmark (alpha=0.05), then the water clarity was considered to be improving and was assigned a value of +1. If less than 30% of the values were significantly below the 30% benchmark, then the water clarity was considered to be degrading and was assigned a value of -1. Non-significant differences were assigned a 0. Similar scores were assigned based on the comparison of the 70th percentiles and the scores summed for each year-segment combination. Combined scores could range from -2 to 2. Scores were computed provided data were available in approximately nine of twelve months. The score from an initial monitoring year of a segment may be biased by an incomplete year of water quality data.

Using the computed scores, categories were assigned to call attention to changing water clarity. Emphasis varied based on whether a segment had been designated as a "Protection" or a "Restoration" segment, recognizing that protection of water clarity required a "hold the line" strategy to maintain ambient conditions, while restoration required an improvement in water clarity. Stability in scores relative to the benchmark period is considered sufficient for the protection targets but not for the restoration targets. The grading system employed (Table 1) assigned both category and color codes.

Results

Overall model calibration of data from 12 segments, evaluated as a LOC between modeled and the highest quality, field-observed K_{dPAR}, was excellent overall, exhibiting a slope of 0.982 and an intercept of -0.002 m^{-1} (Figure 6). The median residual was 0.015 m^{-1}, and the median root mean square error was 0.156 m^{-1}. Over 60% of residuals fell within 0.00±0.20 m^{-1}. The optical model was mechanistically satisfying in that similar attenuation results from similar water quality values in all segments. Not all segments contained sufficient data for a segment-specific assessment of model performance as *n* by segment ranged between 10 and 79, but the median residuals by segment all ranged within 0.000 ± 0.221 m^{-1}, with most between 0.000 ± 0.100 m^{-1}. The two largest median

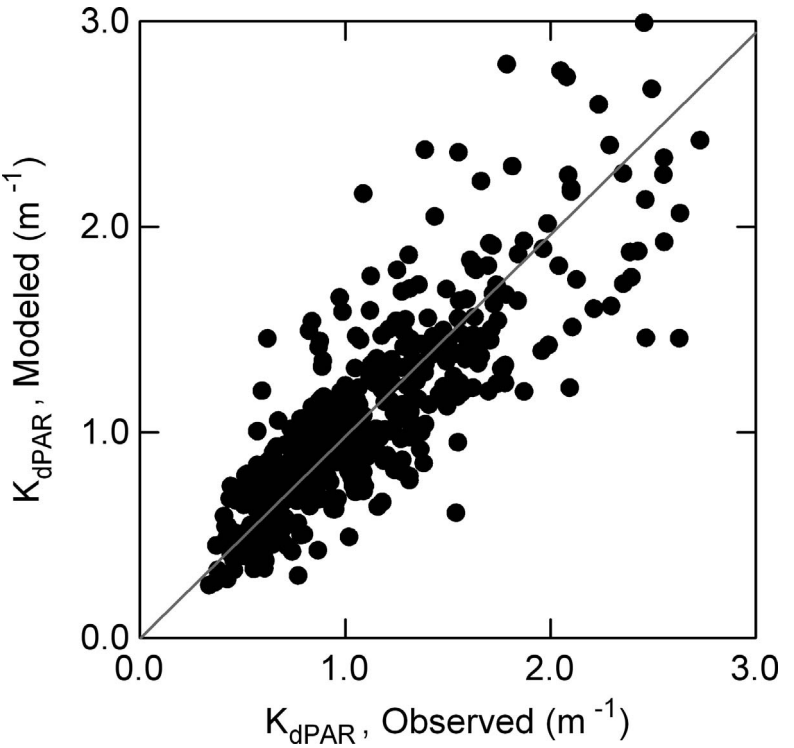

Figure 6. Calibration data of modeled K_{dPAR} as a function of observed (LOC in grey). All segments with the exception of DRB and ULB.

residuals were for the segments with the highest (BOK) and one of the lowest (TPR) water clarities implying that any biases were not due to overall model performance or to the methods of computing partial attenuation coefficients from water quality variables. An independent test of model performance using data from two segments (DRB and ULB) that had not been included in the calibration demonstrated that the optical model was a robust tool with broad regional applicability. The model provides a method of computing water clarity from analyses performed in a controlled laboratory environment, and removes the many uncertainties of field K_{dPAR} measurements, as well as eliminating biases due to the measurement depth dependence of K_{dPAR}, sampling time, varying cloud cover, and bottom type.

For DRB and ULB segments, r^2 criteria were not available to identify the highest quality field K_{dPAR} but maximum observation depths of 0.7 m or greater were selected. As a result, distribution of data for DRB and ULB was larger than that used for model calibration (Figures 7 and 8) and some observations may have been censored if more than two depth observations been available. The LOC of the DRB and ULB data (n=1250), which were not used in model calibration, resulted in a slope of 1.006, an intercept of 0.217 m^{-1}, and median residual of -0.233 m^{-1}, indicating a robustness and broad regional

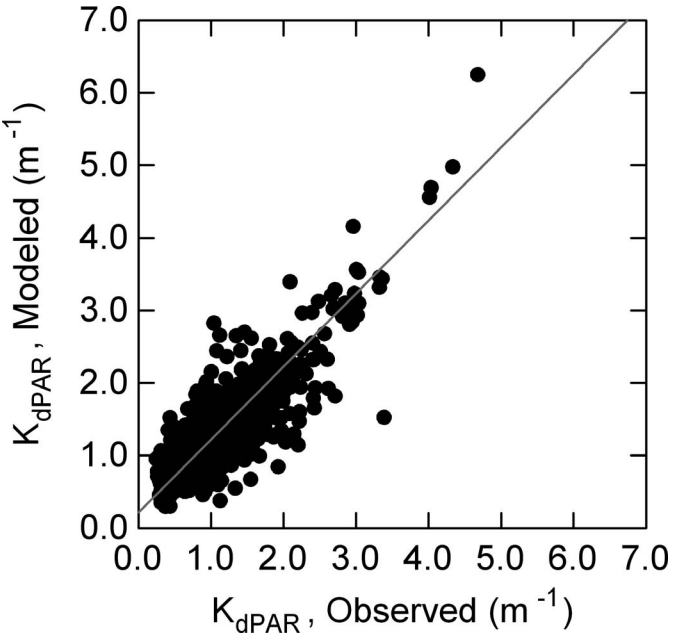

Figure 7. Modeled K_{dPAR} as a function of observed (LOC in grey) for DRB and ULB.

applicability of the empirical optical model. The overestimation of K_{dPAR} in DRB and ULB was primarily associated with higher turbidity levels. These segments are near inlets from the Gulf of Mexico and have periodic, light colored, mineral turbidity associated with coastal wave energy (personal observation). The instances of dominantly mineral turbidity are poorly represented in the data used to derive a_d and would result in a computed a_d

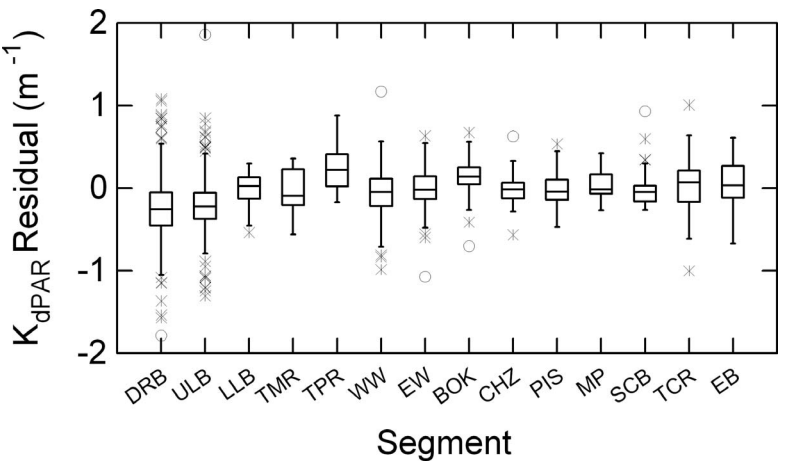

Figure 8. Residuals of K_{dPAR} by segment.

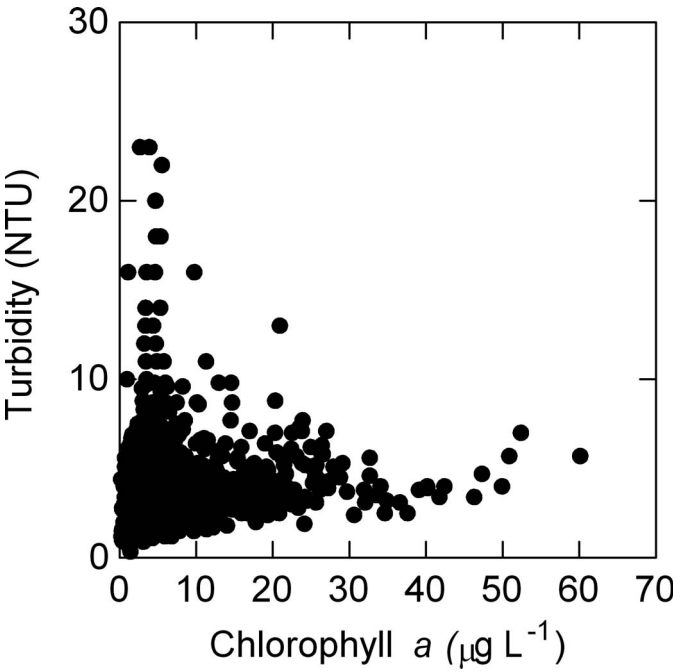

Figure 9. Distribution of turbidity with respect to chlorophyll for DRB and ULB.

biased high (and a model overestimate) relative to the more absorptive, organic particulates of the remaining segments against which model parameters were calibrated. This explanation is further supported by the distribution of elevated turbidity with respect to low chlorophyll concentrations (Figure 9).

Modeled K_{dPAR} values were compiled for the reference period by segment. The benchmark 30^{th} and 70^{th} percentiles were computed (Table 2) and illustrated as a function of target depths (Figure 10). The values of K_{dPAR} as a function of target depth indicated a coherent progression of declining water clarity with declining target depths for all segments of Charlotte Harbor for which high confidence target depths were available. The more riverine segments with poorly defined target depths due to low water clarity exhibited a much larger variation in K_{dPAR} percentiles. Seagrass in these segments typically appears in the more saline regions within the segment, and so the overall segment water clarity, determined from stratified random stations, is likely lower than for the comparatively small region of remaining seagrass.

Annual distributions and percentiles for all years and segments with data were compared to the reference percentiles and scored for significant differences. Annual scores of "Protection" and "Restoration" segments appear in Tables 3 and 4. In addition to segment-specific performance, a number of region-wide trends were evident in the time series of scores. The years of 2001-2003 were often relatively decreased in water clarity, while 2007 was "Stable" or "Improving" in all segments. More recently, clarity declined in many segments in 2010. In 2011,

Table 2. Selected percentiles of the frequency distribution of modeled K_{dPAR} from 2003-2007, target depths, and median %PAR, by seagrass segment.

Segment	Protection (P) Restoration (R)	30th %-ile (m^{-1})	70th %-ile (m^{-1})	Target Depth (m)	Median %PAR
DRB	R	0.90	1.35	1.0	36
ULB	P	0.85	1.17	2.0	14
LLB	R	0.75	1.13	2.0	16
TMR	P	1.47	2.46	0.9	18
TPR	R	1.39	2.41	1.0	15
WW	R	0.87	1.40	1.4	21
EW	R	0.71	1.17	1.4	28
CHZ	P	0.74	1.06	1.9	19
BOK	P	0.56	0.88	2.4	19
PIS	R	0.71	0.98	2.2	16
MP	R	0.62	0.92	2.0	20
SCB	P	0.57	0.91	2.2	22
TCR	R	1.68	2.92	1.0	9
EB	R	0.96	1.39	1.6	18

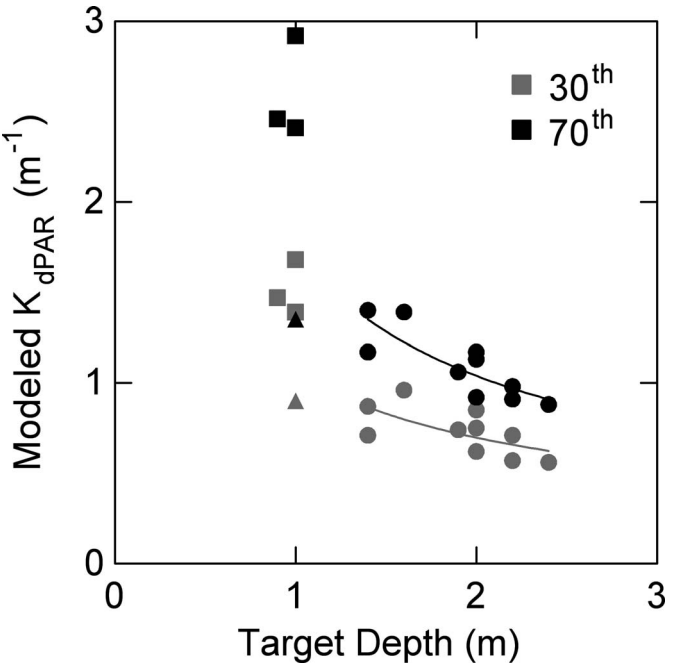

Figure 10. Distribution of 30th (grey) and 70th (black) percentiles of modeled K_{dPAR} with a smooth applied to non-riverine segments (circles) and riverine segments (DRB – triangles; TMR, TPR, TCR – squares).

Table 3. Annual scores for segments with "Protection" designation.

	PROTECTION					
Year	ULB	TMR	BOK	CHZ	PIS	SCB
1998	-2					
1999	-2					
2000	-1					
2001	0	-2		-2		
2002	0	0	-2	-2		2
2003	-1	-2	-2	-2		1
2004	0	0	0	0	0	2
2005	0	-1	-1	0	-1	-1
2006	1	1	0	0	-1	-2
2007	1	2	2	1	2	2
2008	0	0	2	-1	2	0
2009	1	0	1	-1	0	-1
2010	-1	0	0	-1	0	-1
2011	-1	-1	1	-2	0	-1

Table 4. Annual scores for segments with "Restoration" designation.

	RESTORATION							
Year	DRB	LLB	TPR	WW	EW	MP	TCR	EB
1998								
1999								
2000								
2001		-2	-2	-2	-2			
2002		-1	-1	-1	-2		-2	
2003	-2	-1	-2	-2	-2		-2	
2004	0	0	0	0	1	1	0	-1
2005	0	0	-1	-2	-2	-2	-2	0
2006	0	0	0	0	0	0	2	1
2007	2	1	2	2	2	2	2	2
2008	1	-1	0	1	1	0	1	-1
2009	0		-1	-1	-1	0	0	0
2010	-2		-1	1	1	-2	1	-2
2011	-1		0	-1	0	-2	1	-1

there were some improvements over 2010. The segments of ULB, TMR, BOK, and PIS were the segments which recorded the most stable or improving categories over the period of record, consistent with the large areas of seagrasses present in these regions.

The model also provides estimates of %PAR at target depths (Table 2, above) but %PAR values are highly dependent on targets depths (some of which have known uncertainties), and should be interpreted and used with caution. Model assumptions of an optically deep system are implicit and seagrass at target depths undoubtedly receive additional %PAR from bottom reflectance. Due to the exponential relationship between %PAR and K_{dPAR}, transformations between summary K_{dPAR} statistics and %PAR are inappropriate and can

be 70-80% of summary statistics based on individual %PAR data. In addition, due the strong spectral distribution of $K_{d\lambda}$, values of K_{dPAR} only pertain to the depths for which they were modeled; in this case seagrass target depths. For the same water quality, K_{dPAR} can vary by 10-20% when modeled over the range of target depths. Fortunately, model application is straightforward, and target depths readily modified for investigations of potential management actions.

Discussion and Conclusions

Modeled and measured K_{dPAR} measurements often show extensive scatter in their relationship and a discussion of the contributing causes will enhance the appreciation of model calibration results. Most importantly, model formulation is based on simulating optically deep conditions illuminated by direct sunlight only, such that results should be a function of water column attenuators and sun angle alone. However, when PAR measurements at depth are enhanced by bottom reflection (especially noted for scalar PAR sensors), observed K_{dPAR} can be decreased relative to water column attenuation alone (negative residuals). As an apparent optical property, K_{dPAR} is also influenced by the angular distribution of light in addition to the inherent optical properties of absorption and scattering. In shallow, clear waters, bottom reflectance can substantially increase the angular distribution, potentially increasing measured K_{dPAR} (positive residuals). For both low and high solar elevation, if skylight is the dominant contribution to irradiance (early or late day, or overcast), modeled μ_0 based on solar elevation can fail to capture the ambient subsurface angular distribution of light, resulting in either positive or negative residuals. The scatter in individual data points in model calibration represents the potential range of these collective influences.

Much of the Charlotte Harbor estuary is quite shallow, and while model calibration data were censored to obtain field data that were minimally impacted by bottom reflectance, some influence undoubtedly remained. Field data also obviously contain the combined effects of wave climate, skylight, and cloud cover. By calibrating to field data, the optical model implicitly incorporates the mean effects of these factors.

This paper advances previous efforts in deriving empirically based model estimates through the inclusion of techniques for computing $a_{ph\lambda}$ as a function of chlorophyll concentration, using 550 nm as reference wavelengths to compute $a_{g\lambda}$ and $a_{d\lambda}$, and the application of enhancement factors to a_{ph}, a_g and a_d in order to remove the dependence of K_{dPAR} residuals on chlorophyll, color, and turbidity concentrations. Computing $a_{ph\lambda}$ as a series of wavelength-specific power relationships permitted the capture of seasonal variations in accessory pigments that were associated with overall chlorophyll concentrations and possibly with seasonally dominant phytoplankton species. The conventional approach using a^*_{ph440} and a single spectra did not adequately simulate these variations. The use of a mid-spectral reference wavelength for $a_{g\lambda}$ and $a_{d\lambda}$ as used in this work was important for highly absorbing waters with a strong spectral dependence and minimum overall $K_{d\lambda}$ in the mid-spectral region.

Improved precision in the partial absorption coefficients in the mid-spectral region resulted in the largest increase in precision of $I_{z\lambda}$, and consequently the largest increase in precision of K_{dPAR}.

The application of enhancement factors to a_{ph}, a_g and a_d clearly improved model performance across the range of relevant water clarity and water quality parameters. A similar optical model calibrated against field K_{dPAR} (Biber et al. 2008) did not apply enhancements and resulted in model underestimation of 23% for K_{dPAR} values greater than 1.5 m^{-1}. The Charlotte Harbor model, however, was calibrated in the range of 0-3 m^{-1}, useful in this highly colored system, with similar overall accuracies comparable to those described by Biber et al. (2008).

Work in the St. Johns River, another highly colored system (Gallegos 2005), quantified inherent optical properties of absorption and scattering, and partial absorption coefficients as functions of water quality variables, chlorophyll, color, and total suspended solids (TSS). Gallegos' work identified that fine particulates (0.22 – 0.7 μm), roughly proportional to CDOM and likely organic in nature, contributed substantial absorption and scattering but were not included in the direct measurements of a_g or a_d or the resulting relationships with water quality variables. Failing to model the absorptive properties of these fine particulates would result in model underestimates of K_{dPAR} relative to field measured quantities. The Charlotte Harbor system undoubtedly has similar fine organic particulates and the enhancement factors applied to a_d and a_g in this work could be considered to account for these absorptive properties in some measure. The effects of fine particulates were included in the estimates of scattering in the present work (determined as a function of turbidity on unfiltered samples), although variations were observed that were attributed to particulate type (mineral versus organic). There were no independent measures of scattering with which to additionally refine scattering formulations but the model results in this absorption dominated system were relatively insensitive to a variation in scattering of ±15%.

The relationship of $a_{ph\lambda}$ with corrected chlorophyll concentrations, however, should adequately represent both the contributions of typical accessory pigments, as well as the packaging and absorption cross sections associated with typical phytoplankton species without an additional enhancement factor. Review of a_{ph} derivations, indicated modeled a_{ph} less than observed in much of the 20-140 μg L^{-1} chlorophyll range. A repeat of model calibration with no a_{ph} enhancement, indicated an only slightly lower quality model (slope=1.044, intercept of -0.010 m^{-1}) for the 0-88 μg L^{-1} calibration range. From this result, it is apparent that the enhancement factor for chlorophyll affects K_{dPAR} only minimally at low chlorophyll in this high color system, but did improve model agreements at high chlorophyll. The needed enhancement may be attributed to smaller bloom-forming species with higher effective absorption cross sections relative to bulk chlorophyll content.

Although provisions were made to reasonably accommodate water quality data outside of the range used for either determination of partial absorption

coefficients or calibration, the model should be considered an approximation above K_{dPAR} of ~3 m^{-1}. Fortunately, earlier estimates of seagrass requirements as well as the percentiles derived from the modeled K_{dPAR} of this work fall within this range. The lack of a full range of water quality data in the calibration data set was not as problematic as may initially have been perceived.

The use of K_{dPAR}, rather than %PAR, to assess water clarity reduced the sensitivity to selected and possibly uncertain target depths, and the Water Clarity Reporting Tool remains a valid assessment of changes in water clarity over time, even if target depths are not optimum. The optical model and the Water Clarity Reporting Tool combined provide an assessment of changes in water clarity resulting from changes in water column attenuators alone, and a mechanism for the convenient display of results to the general public. Comparisons of future scores to the reference period remain valid only as long as the design frequency and spatial density of the monitoring program remains essentially the same as during which the reference values were developed.

The use of the optical model is not limited to the periodic assessment of water clarity. A versatile tool, it can be applied to other sampling efforts within the Charlotte Harbor region. A highly relevant investigation would be the site-specific modeling with water quality data at the depths of seagrass transects to correlate modeled %PAR and the associated seagrass performance at multi-annual time scales. Application of a similar scoring technique to salinity may help determine the extent to which changes in annual scores are correlated with climatic variations. The Optical Model and the Water Clarity Reporting Tool enhance the ability of the CHNEP to collect and disseminate information relevant to seagrass protection and restoration and to concisely report estuarine conditions to CHNEP constituents.

Acknowledgements Appreciation is due for the long term and continuing efforts of the samplers, analytical staff, and all participants in the Coastal Charlotte Harbor Monitoring Network and the Sarasota County Ambient Monitoring Program, whose data made this project possible. Funding was provided by the Charlotte Harbor National Estuary Program and their many funding partners. Additional thanks are due to reviewers for their detailed and helpful comments.

References

American Public Health Association (APHA). 2005. Standard Methods for Examination of Water & Wastewater: 21st ed. American Public Health Association, Washington D.C.

Arar EJ, Collins GB. 1997. In vitro determination of chlorophyll *a* and pheophytin *a* in marine and freshwater algae by fluorescence. P. 22 *in* National Exposure Research Laboratory, ed. U.S. Environmental Protection Agency, Cincinnati.

American Society for Testing and Materials (ASTM). 2003. ASTM Standard G173 - 03(2003) Standard Tables for Reference Solar Spectral Irradiances: Direct Normal and Hemispherical on 37° Tilted Surface. ASTM International, West Conshohocken.

Austin RW. 1974. The remote sensing of spectral radiance from below the ocean surface. Pp. 317-344 *in* Jerlov NG, Nielssen ES, eds. Optical Aspects of Oceanography. Academic Press, London.

Biber PD, Gallegos CL, Kenworthy WJ. 2008. Calibration of a bio-optical model in the North River, North Carolina (Albemarle – Pamlico Sound): A tool to evaluate water quality impacts on seagrasses. Estuaries and Coasts 31:177-191.

Bricaud A, Morel A, Prieur L. 1981. Absorption by dissolved organic matter of the sea (yellow substance) in the UV and visible domains. Limnology and Oceanography 26:43-53.

Bricaud A, Stramski D. 1990. Spectral absorption coefficients of living phytoplankton and nonalgal biogenous matter: a comparison between the Peru upwelling area and the Sargasso Sea. Limnology and Oceanography 35:562-582.

Buiteveld H, Hakvoort JHM, Donze M. 1994. The optical properties of pure water. Proceedings from Ocean Optics XII. SPIE 2258:174-183.

Butler W. 1962. Absorption of light by turbid materials. Journal of Optical Society of America 52:292-299.

Charlotte Harbor National Estuary Program (CHNEP). 2008. Committing to our future: A comprehensive conservation and management plan for the greater Charlotte Harbor watershed from Venice to Bonita Springs to Winter Haven. Charlotte Harbor National Estuary Program, Fort Myers.

Cleveland JS, Weidemann AD. 1993. Quantifying absorption by aquatic particles: A multiple scattering correction for glass-fiber filters. Limnology and Oceanography 38:1321-1327.

Corbett CA. 2006. Numeric water quality targets for Lemon Bay, Charlotte Harbor and Estero Bay, Florida. Technical Report 06-3. Charlotte Harbor National Estuary Program, Fort Myers.

Corbett CA, Hale JA. 2006. Development of water quality targets for Charlotte Harbor, Florida using seagrass light requirements. Florida Scientist 69(00S2):36-50.

DiToro DM. 1978. Optics of turbid estuarine waters: Approximations and applications. Water Research 12:1059-1068.

Dixon LK. 2000. Establishing light requirements for the seagrass *Thalassia testudinum*: An example from Tampa Bay, Florida. Pp. 9-13 i*n* Bortone, SA, ed. Seagrasses: Monitoring, Ecology, Physiology, and Management. CRC Press, Boca Raton.

Dixon LK. 2014. Old Tampa Bay integrated model development – Task 4 optical model calibration report. Technical Report Number 1732. Mote Marine Laboratory, Sarasota.

Dixon, LK, Kirkpatrick GJ. 1995. Light attenuation with respect to seagrasses in Sarasota Bay, Florida. Mote Marine Laboratory Technical Report No. 407. Sarasota, FL.

Dixon LK, Kirkpatrick GJ. 1999. Causes of light attenuation with respect to seagrasses in upper and lower Charlotte Harbor. Technical Report Number 650. Mote Marine Laboratory, Sarasota.

Dixon LK, Hall ER, Kirkpatrick GJ. 2010. A spectrally explicit optical model of attenuation for Charlotte Harbor seagrasses. Technical Report Number 1460. Mote Marine Laboratory, Sarasota.

Gallegos CL. 1994. Refining habitat requirements of submersed aquatic vegetation: Role of optical models. Estuaries 17(1B):187-199.

Gallegos CL. 2001. Calculating optical water quality targets to restore and protect submerged aquatic vegetation: Overcoming problems in partitioning the diffuse attenuation coefficient for photosynthetically active radiation. Estuaries 24:381-397.

Gallegos CL. 2005. Optical water quality of a black river estuary: The Lower St. Johns River, Florida, USA. Estuarine, Coastal and Shelf Science 63:57-72.

Gallegos C, Correll D, Pierce J. 1990. Modeling spectral diffuse attenuation, adsorption, and scattering coefficients in a turbid estuary. Limnology and Oceanography 35:1486-1502.

Gallegos CL, Lewis EA, Kim HC. 2006. Coupling suspended sediment dynamics and light penetration in the upper Chesapeake Bay. Smithsonian Environmental Research Center, Edgewater.

Gallegos CL, Davies-Colley RJ, Gall M. 2008. Optical closure in lakes with contrasting extremes of reflectance. Limnology and Oceanography 53:2021-2034.

Gallegos CL, Kenworthy WJ, Biber PD, Wolfe BS. 2009. Underwater spectral energy distribution and seagrass depth limits along an optical water quality gradient. Smithsonian Contributions to the Marine Sciences 38:359-367.

Greening HS, Janicki A. 2006. Toward reversal of eutrophic conditions in a subtropical estuary: Water quality and seagrass response to nitrogen loading reductions in Tampa Bay, Florida, USA. Environmental Management 38:163-178.

Helsel DR, Hirsch RM. 2002. Statistical Methods in Water Resources Techniques of Water Resources Investigations. Book 4. Chapter A3. U.S. Geological Survey. http://pubs.usgs.gov/twri/twri4a3/. Accessed March 4, 2016.

Janicki A, Dema M, Wessel M. 2009. Water quality target refinement project – task 2: Seagrass target development. Interim Report 2. Charlotte Harbor National Estuary Program, Fort Myers.

Janicki Environmental Incorporated (JEI). 2009. Water quality targets refinement project task 1: Harbor segmentation scheme. Charlotte Harbor National Estuary Program, Fort Myers.

Janicki Environmental Incorporated (JEI). 2010. Water quality target refinement project - Task 3: Water clarity target development. Interim Report 3. Charlotte Harbor National Estuary Program, Fort Myers.

Janicki Environmental Incorporated (JEI). 2011. Evaluation strategy and reporting tool for CHNEP water clarity targets – Task 3 Supplement. Charlotte Harbor National Estuary Program, Fort Myers.

Johansson JR. 2007. Near-shore water quality and seagrass relationships in the upper portions of Tampa Bay. Pp. 43-48 *in* Corbett C, ed. Colored dissolved organic matter (CDOM) workshop summary. Punta Gorda, Florida May 29-30, 2007.

Johansson JR. 2012. Application of a bio-optical model to determine light availability (PAR) at water depths required to reach the Tampa Bay seagrass restoration goal and at current depths of deep Tampa Bay seagrass meadows. Tampa Bay Estuary Program, Saint Petersburg.

Johansson, JR., Hennenfent KB, Avery WM, Pacowta JJ. 2009. Restoration of seagrass habitat in Tampa Bay using large manatee grass (*Syringodium filiforme*) sod units and a discussion of planting site sediment elevation dynamics. Pp. 153-163 *in* Cooper ST, ed. Proceedings of the Tampa Bay Area Scientific Symposium BASIS5, October 20-23 2009, Saint Petersburg.

Kasten F, Young AT. 1989. Revised optical air mass tables and approximation formula. Applied Optics 28:4735-4738.

Kirk JT. 1981. A Monte Carlo study of the nature of the underwater light field in, and the relationships between optical properties of turbid yellow waters. Australian Journal of Marine and Freshwater Research 32:517–532.

Kirk JT. 1984. Dependence of relationship between inherent and apparent optical properties of water on solar altitude. Limnology and Oceanography 29:350-356.

Kirk JT. 1991. Volume scattering function, average cosines, and the underwater light field. Limnology and Oceanography 36:455-467.

Kirk JT. 1994a. Light and Photosynthesis in Aquatic Ecosystems. Second Edition. Cambridge University Press, Cambridge.

Kirk JT. 1994b. Characteristics of the light field in highly turbid waters: A Monte Carlo study. Limnology and Oceanography 39:702-706.

Kishino M, Takahashi M, Okami N, Ichimura S. 1985. Estimation of the spectral absorption coefficients of phytoplankton in the sea. Bulletin of Marine Science 37:634-642.

McPherson BF, Miller RL. 1994. Causes of light attenuation in Tampa Bay and Charlotte Harbor, southwestern Florida. Water Resources Bulletin 30:43-53

McPherson BF, Miller RL, Stoker YE. 1996. Physical, chemical, and biological characteristics of the Charlotte Harbor basin and estuarine system in southwestern Florida–A summary of the 1982-89 U.S. Geological Survey Charlotte Harbor assessment and other studies. Water Supply Paper 2486. U.S. Geological Survey, Denver.

Mobley CD. 1994. Light and Water: Radiative Transfer in Natural Waters. Academic Press, New York.

Morel A. 1973. Diffusion de la lumière par les eaux de mer; résultats expérimentaux et approche théorique. Pp. 3.1.1-3.1.76 *in* NATO AGARD Lecture Series Number 61 Optics of the Sea, Interface and in-Water transmission and Imaging. September 17-21, 2973, Miami.

Morel A, Gentili B. 1991. Diffuse reflectance of oceanic waters: Its dependence on sun angle as influenced by the molecular scattering contribution. Applied Optics 30:4427-4438.

Mueller JL, Fargion GS, McClain CR, eds. 2003. Ocean optics protocols for satellite ocean color sensor validation - Revision 4, Volume IV: Inherent optical properties: Instruments, characterizations, field measurements and data analysis protocols. NASA/TM-2003-211621/ Rev4-Vol.IV. NASA, Greenbelt.

Nelson NB, Robertson CY. 1993. Detrital spectral absorption: laboratory studies of visible light effects on phytodetritus absorption, bacterial spectral signal, and comparison to field measurements. Journal of Marine Research 51:181-207.

Pope RM, Fry ES. 1997. Absorption spectrum (380–700 nm) of pure water. II. Integrating cavity measurements. Applied Optics 36:8710-8723.

Tomasko DA, Hall MO. 1999. Productivity and biomass of the seagrass *Thalassia testudinum* along a gradient of freshwater influence in Charlotte Harbor, Florida. Estuaries 22:592-602.

Twardowski MS, Boss E, Sullivan M, Donaghay PM. 2004. Modeling the spectral shape of absorption by chromophoric dissolved organic matter. Marine Chemistry 89:69-88.

Wackerly DD, Mendenhall W, Scheeaffer RL. 1996. Mathematical Statistics with Applications 5th Edition. Wadsworth Publishing Company, Belmont.

Wessel MR, Corbett C. 2009. Assessing the performance of an optical model used in setting water quality targets in Lemon Bay, Charlotte Harbor and Estero Bay, Florida. Florida Scientist 72:367-385.

Wessel MR, Beever L, Ott J, Janicki A. 2013 A water clarity evaluation and tracking tool for the estuarine waters of Lemon Bay, Charlotte Harbor and Estero Bay, Florida. Florida Scientist 76:241-248.

Submitted: February 23, 2015
Accepted: March 4, 2016